# UV-Curable Nanocomposites Containing Zirconium Vinylphosphonate or Zirconia

**Lavinia Macarie,[1] Nicoleta Plesu,[1] Smaranda Iliescu,[1] Adriana Popa,[1] Gheorghe Ilia[1,2]**

[1]*Institute of Chemistry Timisoara, Timisoara 300223, Romania*
[2]*Faculty of Chemistry-Biology and Geography, West University, Timisoara 300115, Romania*

Received 28 July 2009; accepted 31 May 2010
DOI 10.1002/app.32881
Published online 23 August 2010 in Wiley Online Library (wileyonlinelibrary.com).

**ABSTRACT:** UV-cured nanocomposite films were prepared from acrylic monomer and two types of nanomaterial: zirconium vinylphosphonate and zirconia, in the presence of a photoinitiator. The films were characterized by FTIR, SEM, and AFM. FTIR spectra showed the disappearance of band assigned to the C=C group both of monomer and zirconium vinylphosphonate by polymerization and the presence of the phosphonate group in polymer. The influence of zirconium vinylphosphonate and zirconia content on thermooxidative degradation of polymeric films was studied by thermogravimetry. SEM and AFM images showed that nanomaterials are dispersed in polymer matrix with no macroscopic phase separation. © 2010 Wiley Periodicals, Inc. J Appl Polym Sci 119: 1820–1826, 2011

**Key words:** nanocomposite; zirconium vinylphosphonate; zirconia; UV-curable resins

## INTRODUCTION

Organic–inorganic polymer nanocomposites have been developed in recent years[1] as new materials with enhanced mechanical properties including hardness, resistance to scratching and abrasion, and high chemical resistance.

Polymer nanocomposite are two phase materials consisting of organic polymeric matrix and inorganic nanosized materials, combining the organic and inorganic characteristics at the molecular level. Therefore, a blending of singular physical properties can be achieved. Nanocomposite materials have successfully been applied in many fields such as protective coatings, plastic processing, optics, electronics, textiles, medicine, etc.

Different metal oxides nanoparticles, such as $SiO_2$, $TiO_2$, ZnO, $CeO_2$,[2–9] $ZrO_2$,[10–13] $Al_2O_3$[14] can be employed as fillers, to obtain nanostructured materials. Also, composite materials were reinforced with clays such as montmorillonites, modified, or unmodified.[15–18]

The morphology and properties of polymer composites depend on the type of incorporated nanoparticles, their size and shape, their concentration, and interactions with the polymer matrix.[19–23]

The nanosized inorganic components are usually incorporated into monomer or polymeric matrices by physically blending. A major problem with nanosized particles is their homogeneous dispersion within the organic matrix avoiding macroscopic phase separation. To obtain a better compatibility between the filler and the host polymeric material and achieve coatings with high content of inorganic particles, the use of coupling agents such as low molecular weight trialcoxysilanes as the precursor for sol–gel reactions is recommended.[24–28]

The organic–inorganic polymer nanocomposites have been prepared by various methods depending on the type of monomers and nanomaterials: bulk polymerization,[29,30] photoinitiated polymerization,[6,10,14,16,17,24,28] emulsion polymerization,[31] *in situ* thermal polymerization,[11,32] or copolymerization in solution,[6,33] by blending the polymer with nanoparticles.[34]

Among these methods, the use of ultraviolet light and photoinitiators to produce polymeric films is one of the most rapid and advantageous method.[35,36]

UV curing technology is attractive from environmental point of view because the photopolymerizable systems are free of organic solvents. Technical advantages are also significant: e.g., low energy consumption and low temperature operation (room temperature) as well as the possibility of curing coatings on sensitive substrates such as wood, paper, and plastics.[37]

In this article, the obtaining and characterization of UV-curable epoxy acrylate polymers as nanocomposite films containing zirconium vinylphosphonate

*Correspondence to:* G. Ilia (ilia@acad-icht.tm.edu.ro or gheilia@yahoo.com).

hybrid material (ZrVP) and zirconia ($ZrO_2$) nanoparticles are reported. The nanomaterials are dispersed in monomer, without covalent bonds[38] in the case of zirconia and with covalent bonds between components in the case of zirconium vinylphosphonate hybrid material, by bonding monomer and vinylphosphonate. The nanocomposite films were characterized by FTIR spectroscopy, SEM, AFM, and thermogravimetric analysis.

## EXPERIMENTAL

### Materials

The starting monomer was an epoxyacrylate oligomer, commercial product as Photomer 3016F (PHA) (Cognis, Monheim, Germany), with high viscosity. For adjusting proper viscosity of this resin, 5 wt % of monomeric diluter trimethylolpropane tryacrylate as Photomer 4006 F (Cognis) was added. Photoinitiator Darocure 4265 containing 50% 2-hydroxy-2-methyl-1-phenyl-propan-1-one and 50% 2,4,6-trimethylbenzoyl-diphenyl-phosphine oxide (Ciba Specialty Chemicals, Basel, Switzerland) was used at 4 wt % versus monomer. As a dispersing agent was used the commercial product Dispersant 182 (Azur SA, Timisoara, Romania), polyglycolether.

$ZrO_2$ (doped with 4% mol $Y_2O_3$) nanoparticles with size lower than 100 nm, synthesized by hydrothermal method, was provided by National Research Institute for Nonferrous and Rare Metals Bucharest. Zirconium vinylphosphonate (ZrVP) hybrid material was obtained by hydrothermal method according to Ref. 39 and 40 at nanosized scale.

### Curing procedure

The various photopolymerizable formulations were obtained from monomer, photoinitiator, and nanomaterial. The nanomaterial was dispersed in the dispersing agent and added to the liquid monomer at 5, 10, and 15% content,versus monomer mass, using ultrasonic bath at 35°C. The formulation was laid on glass panel and PTFE plates using a film applicator to obtain film of about 100 μm. The wet films were exposed to medium-pressure mercury vapour lamp (maximum power 120 W $cm^{-1}$, belt speed 3 m $min^{-1}$), at room temperature.

### Characterization

Fourier transform infrared spectra (FTIR) of the monomer and polymers were recorded, using Model Jasco FT/IR-4200 apparatus, in KBr pellet, following the band attributable to the phosphonic groups and decrease of the band attributable to the C=C group, due to the polymerization.

**TABLE I**
**Polymer Content of Nanocomposite Films**

| Film | Gel content (%) |
|---|---|
| PHA | 98.10 |
| ZrVP-PHA 5% | 96.50 |
| ZrVP-PHA 10% | 94.83 |
| ZrVP-PHA 15% | 91.51 |
| $ZrO_2$-PHA 5% | 96.46 |
| $ZrO_2$-PHA 10% | 93.74 |
| $ZrO_2$-PHA 15% | 94.48 |

The gel content was determined on cured films by measuring the mass loss after 24 h extraction with dichloromethane.

The cured nanocomposite films were analyzed by TGA to record their thermal stability at different content of nanomaterial, using TGA/SDTA 851-LF 1100-Mettler aparatus, in the presence of air, with a heating rate 10°/min from ambient temperature to 750°C.

SEM analyses were performed using Inspectes apparatus, and AFM images were performed by Nanosurf easy Scan 2 Advanced Research AFM, to investigate the homogeneity of the coatings.

The pendulum hardness was evaluated on photocured films with Koenig pendulum according with ASTM D4366-95.

## RESULTS AND DISCUSSION

The photoinitiator Darocure 4265 produced after UV-irradiation radicals able to react with C=C group, both of the monomers and ZrVP, to yield an insoluble network. Thus, the ZrVP is incorporated into the network by chemical bonding. The photocured films are characterized by a high gel content values (Table I) indicating the formation of almost completely insoluble network and therefore confirming the efficiency of UV-initiated polymerization.

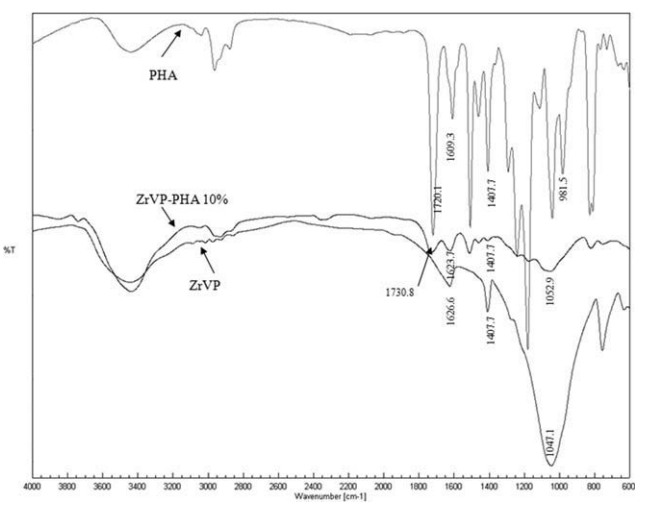


**Figure 1** FTIR spectra of monomer PHA, ZrVP, and polymer ZrVP-PHA 10%.

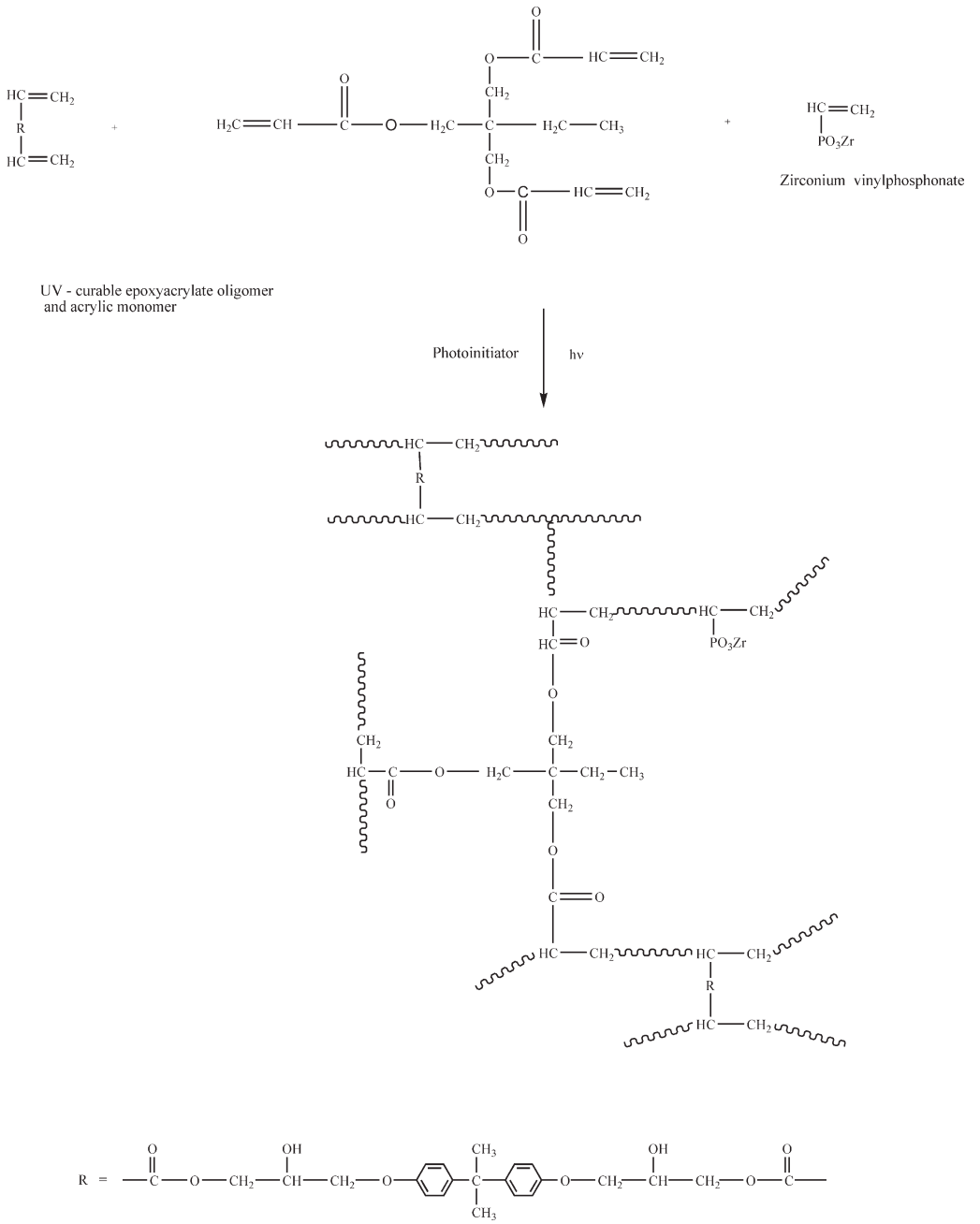


**Scheme 1** Copolymerization of acrylic monomers with zirconium vinylphosphonate.

## IR spectra of the films

In Figure 1, the spectra of the monomer PHA, ZrVP, and polymer ZrVP-PHA 10% are shown. The monomer presents absorption bands at 1609.3 $cm^{-1}$, 1407.7 $cm^{-1}$, and 981.5 $cm^{-1}$ assigned to the C=C group and at 1720.1 $cm^{-1}$ to C=O of acrylate.[41]

The absorption at 1047.1 $cm^{-1}$ is attributed to the phosphonate group of ZrVP.[42] The absorption at 1626.6 $cm^{-1}$ and 1407.7 $cm^{-1}$ are assigned to C=C group in ZrVP.

The FTIR spectrum of the polymeric film ZrVP-PHA 10% showed the decrease of the absorption bands attributed to C=C, because the polmerization occured. The presence of absorption band assigned to phosphonate group at 1052.9 $cm^{-1}$ and to C=O group at 1730.8 $cm^{-1}$ are also identified. The possible chemistry[43] related in the polymeric films can be revealed by Scheme 1.

## Thermal properties of the films

Figure 2 shows TG-DTA curves of the pure PHA polymer film and films containing ZrVP of 5, 10, and 15% content, in dry air, from room temperature to 750°C.

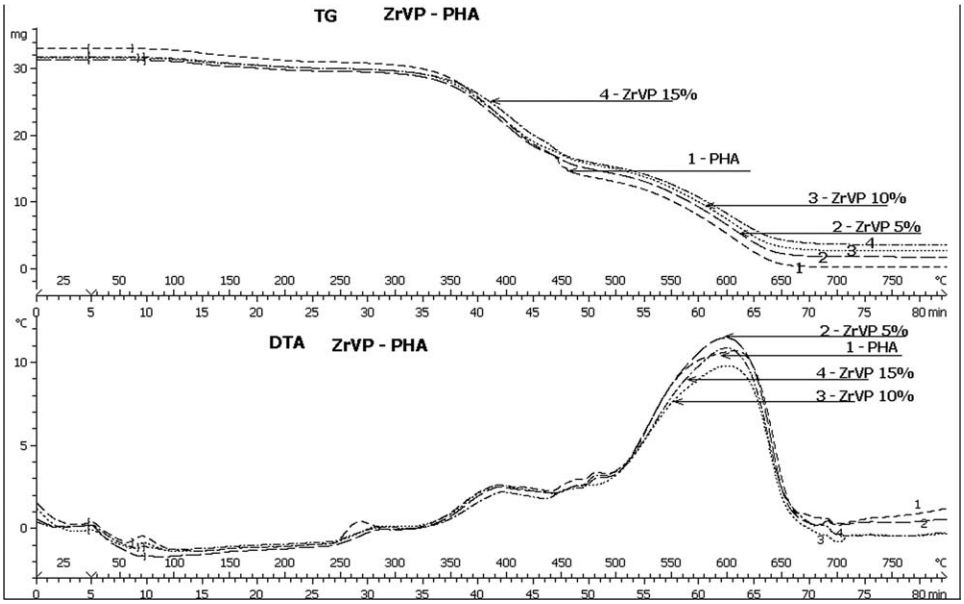


**Figure 2** TG-DTA curves of thermal analysis of films containing ZrVP at 5, 10, and 15% content in comparison with PHA polymer.

The thermal behavior of PHA, ZrVP-PHA and $ZrO_2$-PHA at different nanomaterial content can be divided in three regions.

Also, we selected the temperature when the 5% mass is lost ($T_{d\text{-}5\%}$) as a comparison point.

For PHA film, it can be observed that the first region is from room temperature to 308.2°C, when a small mass loss of around 8.2% occured. This can be attributed to the desorption of humidity, removal of unreacted monomers, and structural decomposition of the epoxy groups from monomer.[44]

The second region is in the temperature domain between 308.2°C and 441.3°C, when a major mass loss of 39.5% is observed, due to the decomposition of polymer. The third region is between 441.3°C and 710.3°C with another major mass loss of 52% attributed to the degradation of the polymeric chain by a complex oxidative processes. Practically, it can be assumed that the polymer PHA is stable till 308.2°C, and the decomposition occurs above this temperature.

The results of thermal behavior of nanocomposites are presented in Table II.

In the case of films with ZrVP and $ZrO_2$ content, the first region of thermograms shows the low mass loss in the range of 6.5–8%, attributed to the removal of dispersant, unreacted monomers, or humidity.

In comparison with PHA polymer, the glass transition temperatures of the nanocomposites increased, especially in the case of $ZrO_2$-PHA when $T_g$ were significantly enhanced (Table II).

In the case of ZrVP-PHA polymer, we assume that the enhanced glass transition temperatures resulted from the restricted motion of the polymer chains that was caused by the random polymerization of the ZrVP units in the polymer chain.[45]

In the case of $ZrO_2$-PHA nanocomposites, it can be observed the unexpected decrease of the $T_g$ as loading is more. This $T_g$ depression is in accordance with literature data[46] and could be attributed to the influence of the increased content of the low molecular weight species.

In the case of ZrVP-PHA nanocomposites, only a slight increase of decomposition temperatures $T_{dec1}$ and $T_{dec2}$ was noticed, although the polymerization of ZrVP in polymer chain was occured. This may be

**TABLE II**
**TGA Data for the UV-Cured Nanocomposites**

| Sample | $T_g$ (°C) | $T_{d\text{-}5\%}$ (°C) | $T_{dec\ 1}$ (°C) | Mass loss (%) | $T_{dec2}$ (°C) | Mass loss (%) | Reziduu (%) |
|---|---|---|---|---|---|---|---|
| PHA | 56.2 | 184.7 | 308.2 | 39.5 | 441.3 | 52 | 0.3 |
| ZrVP-PHA 5% | 63.4 | 197.9 | 309.9 | 39.1 | 446.2 | 48.4 | 5.2 |
| ZrVP-PHA 10% | 60.9 | 232.3 | 310.0 | 38.5 | 448.7 | 46.5 | 8.2 |
| ZrVP-PHA 15% | 62.6 | 234.1 | 313.3 | 33.7 | 445.2 | 47.8 | 10.9 |
| $ZrO_2$-PHA 5% | 78.5 | 228.3 | 309.9 | 39.3 | 440.4 | 48.8 | 5.02 |
| $ZrO_2$-PHA 10% | 62.3 | 246.8 | 300.5 | 37.0 | 436.3 | 49.3 | 7.57 |
| $ZrO_2$-PHA 15% | 57.5 | 271.6 | 310.7 | 37.8 | 439.1 | 44.4 | 11.3 |

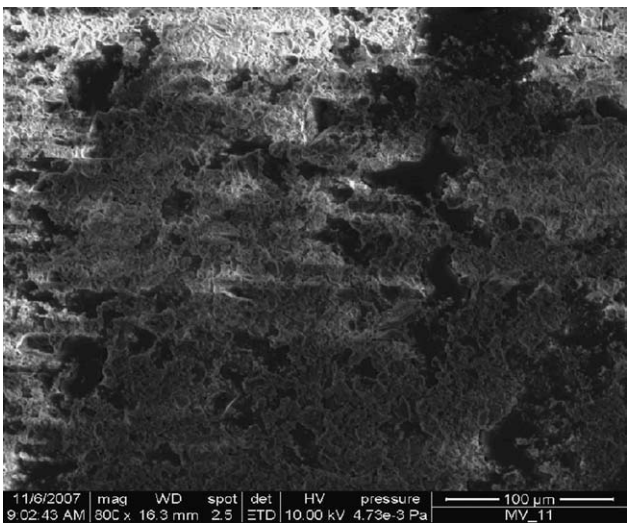


**Figure 3** SEM image of the ZrVP.

due to the presence of organic functional group in the ZrVP molecule that has low decomposition temperature (<310°C).

The uneven variation of decomposition temperatures $T_{dec1}$ and $T_{dec2}$ of nanocomposites containing $ZrO_2$ can be explained by the influence of two factors which have opposite influences on the thermal behavior.

First, the addition of inorganic material like zirconium oxide decreases the curing reactivity of epoxy resin. When the resin has a lower reactivity, it results a lower crosslinking density of the cured resin and the longer polymer chains among the crosslinking points. Also, it is known that a longer polymer chain is less stable thermally than a shorter chain,[21] so the nanocomposites are easier to degrade than the neat epoxyacrylate resin. The second factor reffers to the fact that the decomposition temperature increases with the increase of inorganic material content. Hence, for 5% content of $ZrO_2$, the decomposition temperature of 309.9°C is close to the polymer PHA decomposition temperature of 308.2°C, because the influence of the inorganic amount predominates the influence of the decrease crosslinking density.

In the case of 10% content, the influence of the decrease of crosslinking density could not be overcome by the influence of the increase of $ZrO_2$ content, and, as a result, the decomposition temperature decreases to 300.5°C. This is also supported by the solubility results (Table I). The gel content decrease from 96.46% for 5% to 93.74% for 10% $ZrO_2$.

For 15% $ZrO_2$ content, the decomposition temperature increases to 310.7°C, because in this case, the higher content of inorganic material overcomes the influence of the decrease of the crosslinking density.

Therefore, by adding ZrVP and $ZrO_2$ to epoxyacrylate resin, the thermal behavior of the obtained nanocomposites showed an increase of temperature when 5% mass loss occured in comparison with neat polymer. The decomposition temperatures of the epoxyacrylate nanocomposites are slightly influenced by addition of nanomaterials at different content.

## Appearance of the films

By visual investigation, the ZrVP-PHA films are colourless and transparent, and $ZrO_2$-PHA films are relatively opalescent, that means the formation of the homogeneous phase between organic and inorganic components. The film were very adhesive on the glass plates, but not on the PTFE plates from which they can be peeled and analyzed.

Figure 3 shows the SEM images of ZrVP, which presents a homogeneous texture.

Figure 4(a,b) shows the SEM images of the polymeric film of PHA containing 5% ZrVP (a) and 5% $ZrO_2$ (b), respectively. The film containing ZrVP,

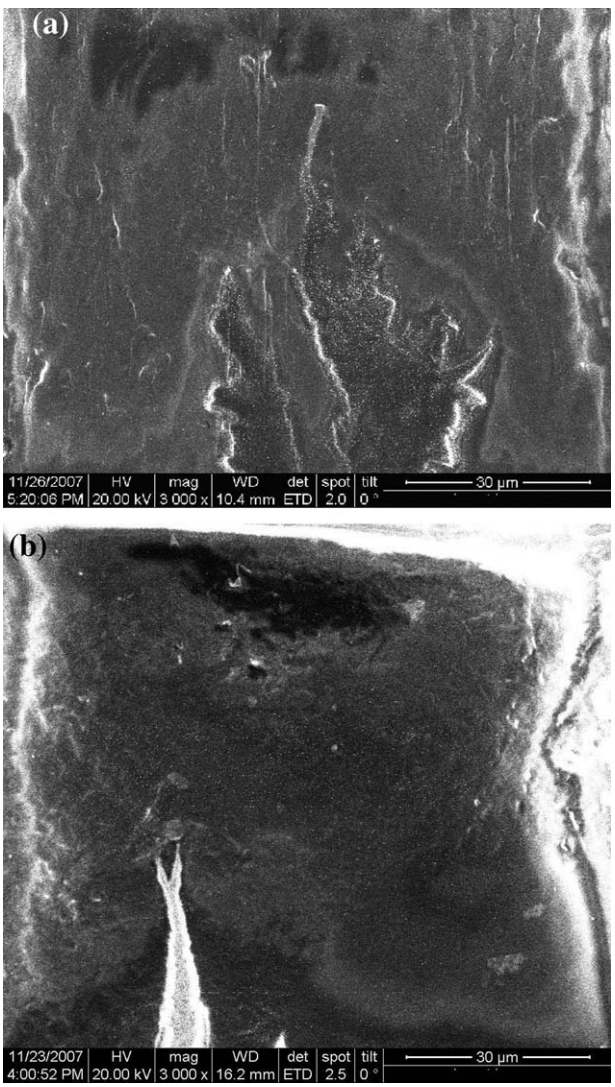


**Figure 4** (a) SEM image of the film containing ZrVP-PHA 5%. (b) SEM image of the film containing ZrO2-PHA 5%.

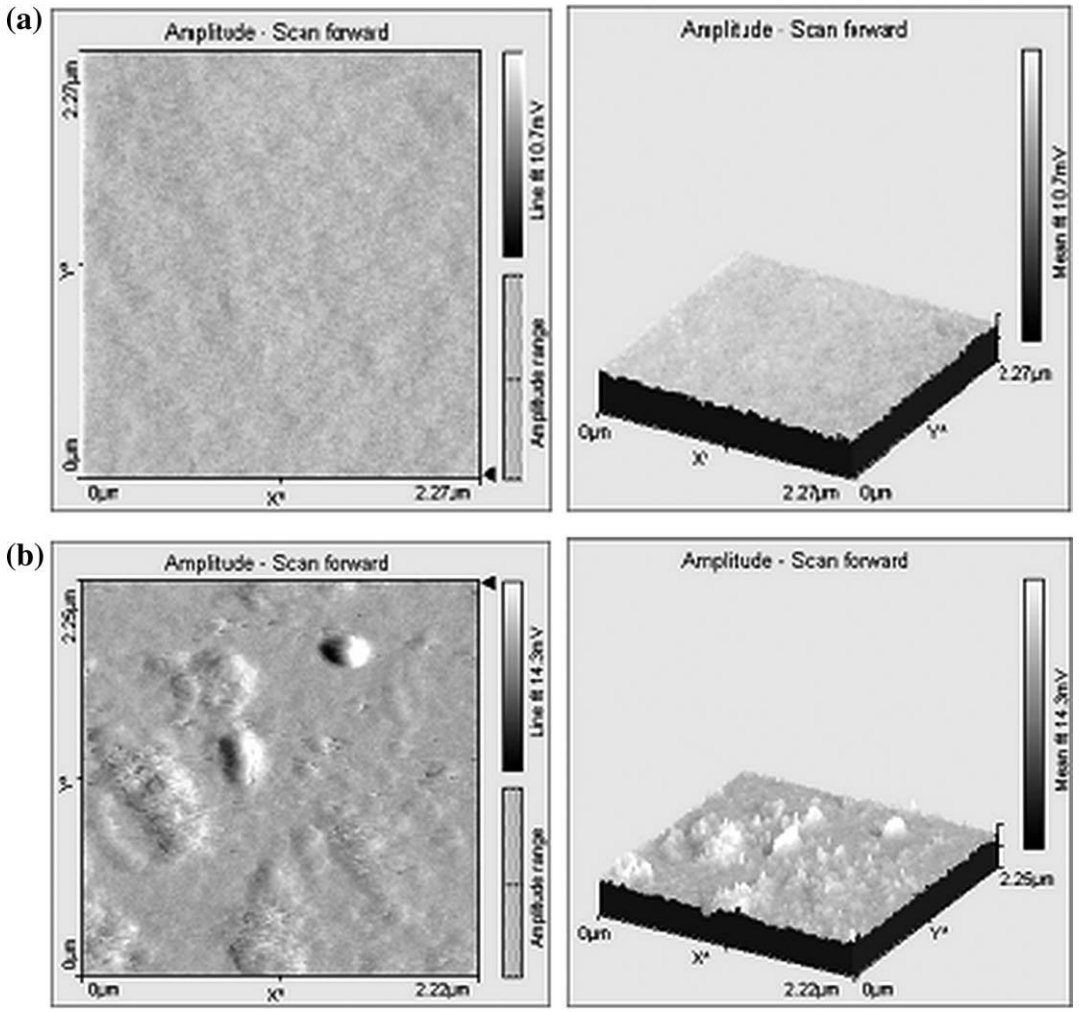


**Figure 5** (a) AFM images at 2.3 × 2.3 μm$^2$ surface of the films ZrVP-PHA 5%. (b) AFM images at 2.3 × 2.3 μm$^2$ surface of the films ZrO2-PHA 5%.

which is chemical bonded to polymer, has a dense and more homogeneous structure in comparison with the film containing $ZrO_2$, where the inorganic nanoparticles are physically included in polymer matrix.

Figure 5(a,b) shows the AFM images of ZrVP-PHA 5% (a) and $ZrO_2$-PHA 5% (b) films. The images show that the organic and inorganic phases are dispersed, with no macroscopic phase separation. The film containing ZrVP is more homogeneous than film containing $ZrO_2$; in the latter case, the inorganic material is uniformly embedded in the polymer matrix on nanometric scale.

### Mechanical film properties

The Koenig pendulum hardness test measured the surface hardness of the films laid on glass panel (Fig. 6). By adding ZrVP and $ZrO_2$, the film hardness increased in comparison with PHA film. The film containing 15% ZrVP presents a moderately lower hardness in comparison with 5% and 10% content. Although the thermal analysis showed that the $ZrO_2$-PHA polymeric films have lower thermal stability, however, the values of the pendulum hardness are higher than ZrVP-PHA films due to the intrinsic hardness of $ZrO_2$.

## CONCLUSIONS

Transparent ZrVP-PHA and opalescent $ZrO_2$-PHA nanocomposite films were prepared by photoinitiated polymerization (photoinitiator Darocure 4265) of formulations containing epoxyacrylate oligomer and Zr-vinylphosphonate or $ZrO_2$ nanomaterials at different content. The FTIR spectra suggested that zirconium vinylphosphonate was covalent bonded to monomer to form a cross-linked network polymer (by disappearance of the band assigned to C=C around 1400 cm$^{-1}$). SEM and AFM images showed that zirconium phosphonate hybrid and inorganic

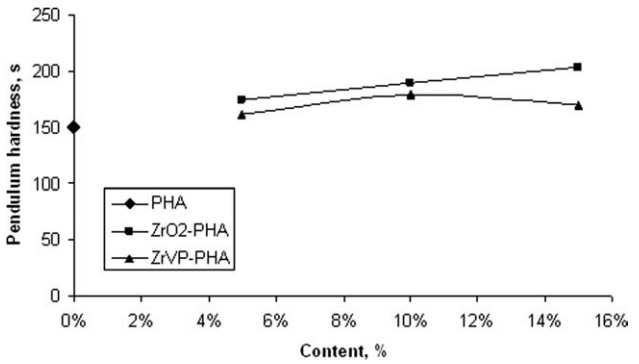


**Figure 6** Results of pendulum hardness test.

zirconia nanomaterials were homogeneously dispersed within the polymer matrix. TG measurements showed that increase of the ZrVP content in nanocomposite led to a slight increase of decomposition temperatureversus PHA polymer films. The presence of zirconia decreased the decomposition temperature in comparison with PHA polymer but enhanced the mechanical property of the film with 26%. However, the increase of nanomaterial content in polymer matrix can enhance the thermal stability untill the temperature when 5% mass loss occured.

## References


1. Herr, D.; Chaplinsky, S.; Romanelli, A. L.; Zadjura, R. J Appl Polym Sci 2008, 107, 3244.
2. Tianbin, W.; Yangchuan, K. Polym Degrad Stab 2006, 91, 2205.
3. Reck, E.; Seymour, S. Macromol Symp 2002, 187, 707.
4. Sangermano, M.; Malucelli, G.; Amerio, E.; Priola, A.; Billi, E.; Rizza, G. Prog Org Coat 2005, 54, 134.
5. Lu, N.; Lu, X.; Jin, X.; Lu, C. Polym Int 2006, 56, 138.
6. Wan, T.; Feng, F.; Wang, Y. C. Polym Bull 2006, 56, 413.
7. Dong, C.; Ni, X. J Macromol Sci Part A Pure Appl Chem 2004, A41, 547.
8. Butler, L.; Cammarano, R.; Lee, D.; McCormick, P. G.; Tsuzuki, T. Proceedings of XXVII FATIPEC Congress. XXVII FATIPEC Congress, Aix-en-Provence, France; Lemercier, R.; Revillon, A. Eds. Wiley-VCH Verlag, Weinheim, Germany 2004; 121.
9. Shu, C. H.; Chiang, H. C.; Tsiang, R. C. C.; Liu, T. J.; Wu, J. J. J Appl Polym Sci 2007, 103, 3985.
10. Nakayama, N.; Hayashi, T. Composites 2007, A 38, 1996.
11. Wang, H.; Xu, P.; Zhong, W.; Shen, L.; Du, Q. Polym Degrad Stab 2005, 87, 319.
12. Simon, P.; Zhong, W.; Bakos, D.; Hynek, D. Chem Pap 2008, 62, 176.
13. Chang, T. C.; Wang, Y. T.; Hong, Y. S.; Chiu, Y. S. Thermochim Acta 2002, 390, 93.
14. Landry, V.; Riedl, B.; Blanchet, P. Prog Org Coat 2008, 61, 76.
15. Alexandre, M.; Dubois, P. Mater Sci Eng 2000, R28, 1.
16. Uhl, F. M.; Webster, D. C.; Davuluri, S. P.; Wong, S. C. Eur Polym J 2006, 42, 2596.
17. Fogelstrom, L.; Antoni, P.; Malmstrom, E.; Hult, A. Prog Org Coat 2006, 55, 284.
18. Lewicki, J. P.; Liggat, J. J.; Patel, M. Polym Degrad Stab 2009, 94, 1548.
19. Palza, H.; Vergara, R.; Yazdani-Pedram, M.; Quijada, R. J Appl Polym Sci 2009, 112, 1278.
20. Dufresne, A.; Paillet, M.; Putaux, J. L.; Canet, R.; Carmona, F.; Delhaes, P.; Cui, S. J Mater Sci 2002, 37, 3915.
21. Pandey, J. K.; Reddy, K. R.; Kumar, A. P.; Singh, R. P. Polym Degrad Stab 2005, 88, 234.
22. Utracki, L. A.; Sepehr, M.; Boccaleri, E. Polym Adv Technol 2007, 18, 1.
23. Khrenov, V.; Schwager, F.; Klapper, M.; Koch, M.; Mullen, K. Polym Bull 2007, 58, 799.
24. Malucelli, G.; Priola, A.; Sangermano, M.; Amerio, E.; Zini, E.; Fabbri, E. Polymer 2005, 46, 2872.
25. Sangermano, M.; Acosta, O. R.; Garcia Valdez, A. E.; Berlanga Duarte, L.; Amerio, E.; Priola, A.; Rizza, G. Polym Bull 2008, 59, 865.
26. Wan, T.; Lin, J.; Li, X.; Xiao, W. Polym Bull 2008, 59, 749.
27. Nakane, K.; Kurita, T.; Ogihara, T.; Ogata, N. Compos B Eng 2004, 35, 219.
28. Decker, C.; Zahouily, K.; Keller, L.; Benfarhi, S.; Bendaikha, T.; Baron, J. J Mater Sci 2002, 37, 4831.
29. Pattanayak, A.; Jana, S. C. Polymer 2005, 46, 3275.
30. Demir, M. M.; Memesa, M.; Castignolles, P.; Wegner, G. Macromol Rapid Commun 2006, 27, 763.
31. Park, B. J.; Kim, T. H.; Choi, H. J.; Lee, J. H. J Macromol Sci Part B 2007, 46, 2.
32. Dai, C. F.; Li, P. R.; Yeh, J. M. Eur Polym J 2008, 44, 2439.
33. Zhao, C.; Yang, X.; Wu, X.; Liu, X.; Wang, X. Polym Bull 2008, 60, 4.
34. Xiong, M.; Gu, G.; You, B.; Wu, L. J Appl Polym Sci 2003, 90, 7.
35. Feng, L.; Suh, B. I. J Appl Polym Sci 2009, 112, 1565.
36. Tan, H.; Yang, D.; Xiao, M.; Han, J.; Nie, J. J Appl Polym Sci 2009, 111, 1936.
37. Dietliker, K.; Crivello, J. V. Chemistry and Technology of UV and EB Formulation for Coatings, Inks and Paints; Bradley, G.; Ed.; John Wiley and Sons/SITA Technology: London, 1998; Vol. 3.
38. Mark, J. E.; Wang, S.; Xu, P.; Wen, J. Mater Res Soc Symp Proc 1992, 274, 77.
39. Beck, S.; Brough, A. R.; Bochmann, M. J Mol Catal A Chem 2004, 220, 275.
40. Knight, D. A.; Kim, V.; Raymond, J.; Butcher, R. J.; Brandy, A.; Harper, B. A.; Schull, T. L. J Chem Soc Dalton Trans 2002, 824.
41. Bacaloglu, R.; Csunderlik, C.; Cotarca, L.; Glatt, H. H. Structure and Properties of Organic Compounds (Structura si Proprietatile Compusilor Organici); Technical: Bucharest, 1985; Vol. I.
42. Thomas, L. C. Interpretation of the Infrared Spectra of Organophosphorus Compounds; Heyden: London, 1974.
43. Imamoglu, T.; Yagci, Y. Turk J Chem 2001, 25, 1.
44. Musto, P.; Ragosta, G.; Russo, P.; Mascia, L. Macromol Chem Phys 2001, 202, 3445.
45. Goldman, M.; Shen, L. Phys Rev 1966, 144, 321.
46. Lin, H. C.; Kuo, S. W.; Huang, C. F.; Chang, F. C. Macromol Rapid Commun 2006, 27, 537.